chemosensors

MDPI

Supporting Information

Dual-Response Photofunctional Covalent Organic Framework for Acid Detection in Various Solutions

Wenyue Ma [1], Zijian Gu [1], Guocui Pan [1], Chunjuan Li [2], Yu Zhu [2], Zhaoyang Liu [1], Leijing Liu [1], Yupeng Guo [2], Bin Xu [1] and Wenjing Tian [1,*]

[1] State Key Laboratory of Supramolecular Structure and Materials, College of Chemistry, Jilin University, Changchun 130012, China; wenyue20@mails.jlu.edu.cn (W.M.); zjgu20@mails.jlu.edu.cn (Z.G.); pangc20@mails.jlu.edu.cn (G.P.); zhaoyangliu@jlu.edu.cn (Z.L.); liuleijing@jlu.edu.cn (L.L.); xubin@jlu.edu.cn (B.X.)

[2] National Chemistry Experimental Teaching Demonstration Center, Jilin University, Changchun 130012, China; licj1219@mails.jlu.edu.cn (C.L.); zhuyu1220@mails.jlu.edu.cn (Y.Z.); guoyupeng@jlu.edu.cn (Y.G.)

* Correspondence: wjtian@jlu.edu.cn

Synthetic procedures

1. The synthetic method of TPBD-TA COF was modified according to previous literature [1]. TPBD (23.2 mg) and TA (13.4 mg) were mixed in the presence of o-Dichlorobenzene / n-BuOH / 6 M AcOH (5/5/1 by vol.; 2.2 mL) in a Pyrex tube (10 mL), which was degassed by three freeze-pump-thaw cycles. The tube was sealed off and heated at 120 °C for 3 days. The production was collected by centrifugating and washing with anhydrous THF five times and acetone three times. The resulting powder was a red powder.

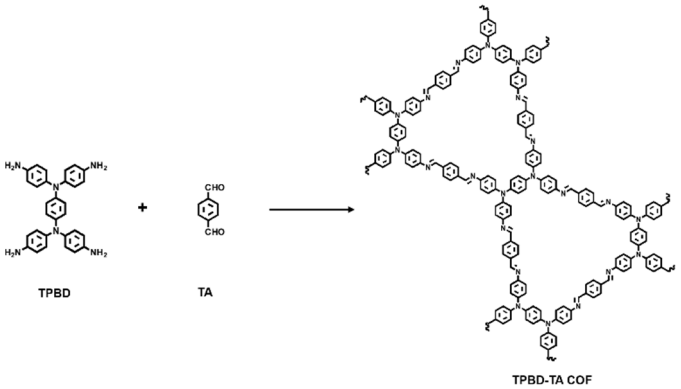

Figure S1. Synthesis route of TPBD-TA COF.

2. Model compounds were synthesized according to a reported procedure with some modifications [2]. Firstly, acetic acid (25 μL) was added to N, N, N′, N′-tetrakis(4-aminophenyl)-1,4-phenylenediamine (472.58 mg) and benzaldehyde (450 μL) in ethanol (15 mL). The reaction was then stirred at 50 °C for 12 h. When cooled to room temperature, the solid was collected by filtration and washed with H_2O, ethanol and CH_2Cl_2. The pure yellow product was obtained after removing the solvent under vacuum at room temperature. ^1H NMR (500 MHz, $CDCl_3$) δ 8.52 (s, 4H), 7.90 (dd, J = 6.6, 2.8 Hz, 8H), 7.49 – 7.44 (m, 13H), 7.21 (d, J = 8.8 Hz, 8H), 7.17 (d, J = 8.9 Hz, 8H), 7.06 (s, 4H).

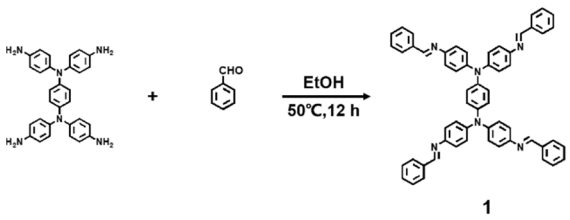

Figure S2. Synthesis route of the model compound **(1)**.

Experimental details

1. Information encryption test

The "JLU" pattern was written on the COF filter paper by 0.1 mmol L^{-1} TFA, then the filter paper was fumed in the closed container with NH_3 vapor until the pattern disappeared. Lastly, the filter paper was heated for a several minutes until the letter pattern appeared again.

2. Theory calculations

All the density functional theory (DFT) calculations were carried out using Gauusian 09 package on a PowerLeader clusters [2]. The natural transition orbitals (NTOs) and corresponding energy levels of the TPBD-TA COF fragment, based on the time-dependent density functional theory (TD-DFT), were fully calculated by using m062x/6-31G (d, p).

3. Molecular simulation

The lattice model was optimized through using the Materials Studio Forcite molecular dynamics module under ultra-fine, Universal force fields, Ewald summations condition to determine the structure of TPBD-TA COF. Then Pawley refinement was conducted using Reflex to fit profile of PXRD.

Supplementary Figures

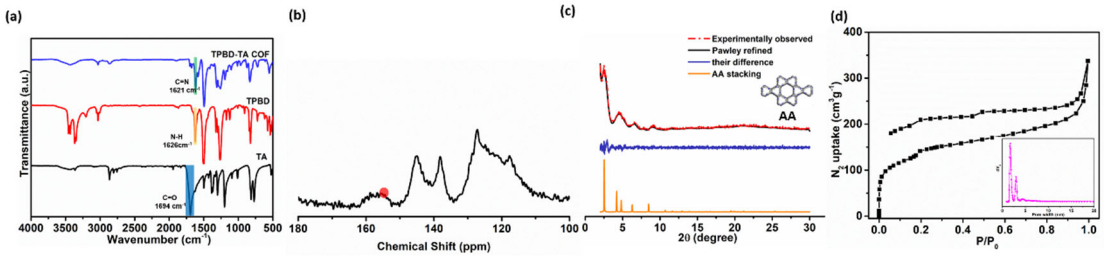

Figure S3. (a) FT IR spectra of TPBD-TA COF, (b) Solid-state ^{13}C NMR spectrum of TPBD-TA COF, (c) PXRD patterns of TPBD-TA COF of the experimentally observed (red), Pawley refined (black) and their difference (blue), simulated using the AA (yellow) stacking mode, (d) N_2 adsorption/ desorption isotherms of TPBD-TA COF (inset: pore size distribution of TPBD-TA COF powders).

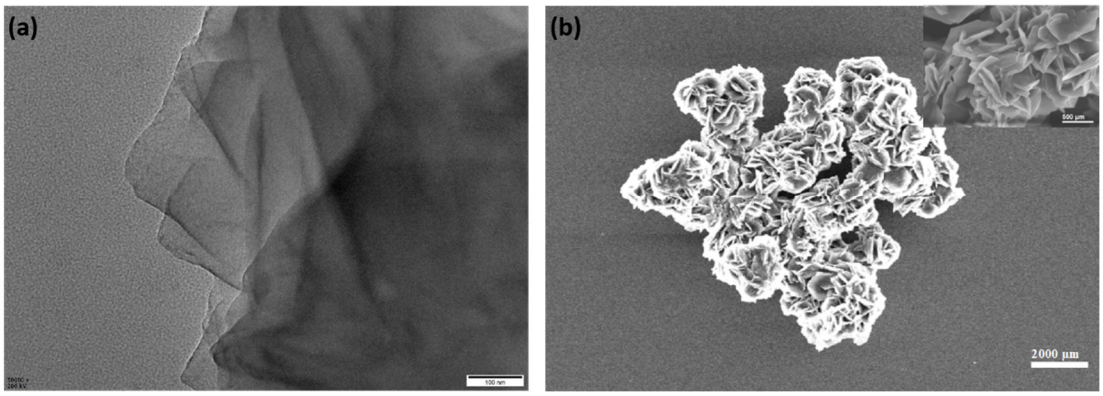

Figure S4. (a) TEM image of TPBD-TA COF, (b) SEM images of TPBD-TA COF.

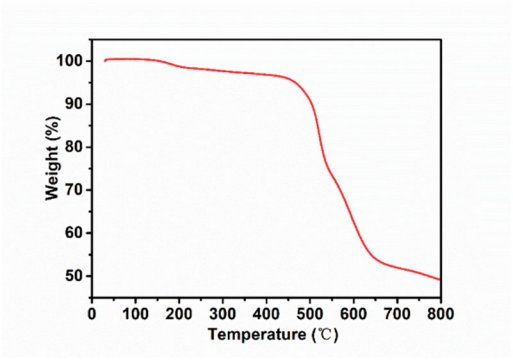

Figure S5. TGA curve of TPBD-TA COF.

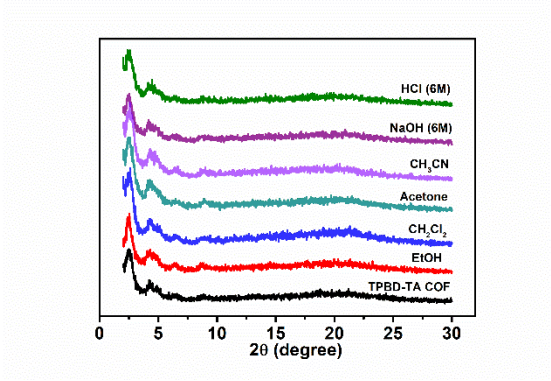

Figure S6. PXRD patterns of TPBD-TA COF after immersion in various solvents for 48 h.

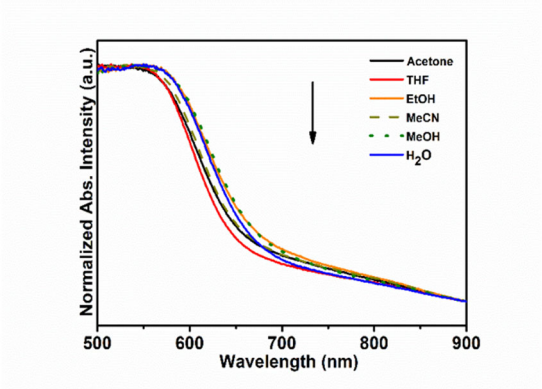

Figure S7. Solid-state absorption spectra of TPBD-TA COF in different solvents.

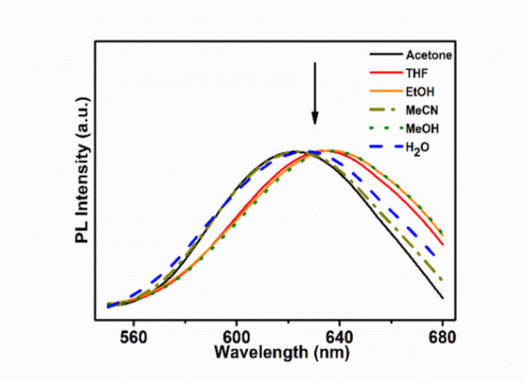

Figure S8. Fluorescence spectra of TPBD-TA COF in different solvents.

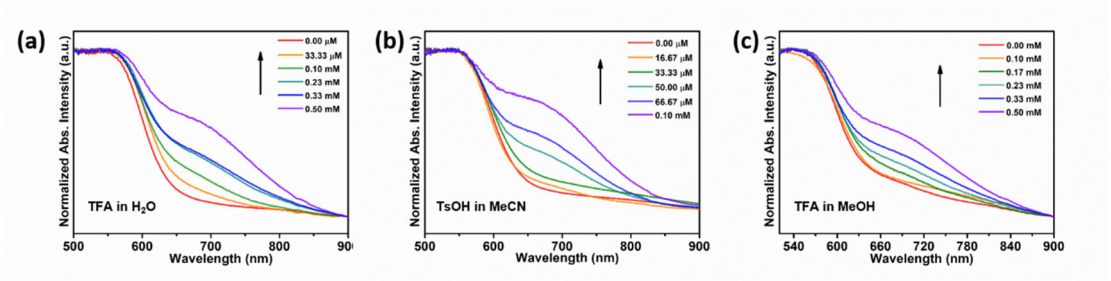

Figure S9. Solid-state absorption spectra of TPBD-TA COF in (a) trifluoroacetic acid (TFA) aqueous solution, (b) 4-methylbenzenesulfonic acid (TsOH) in MeCN solution, (c) TFA in MeOH solution with different acid.

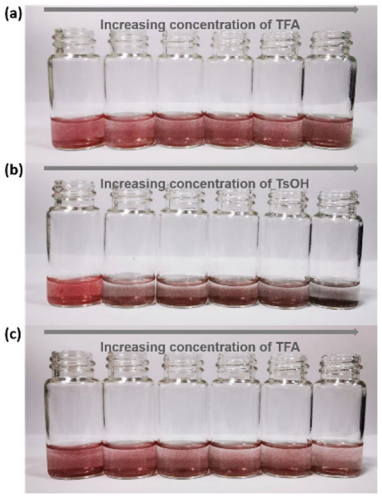

Figure S10. Color changes of TPBD-TA COF in increasing concentrations of (a) TFA in water, (b) TsOH in MeCN and (c) TFA in MeOH.

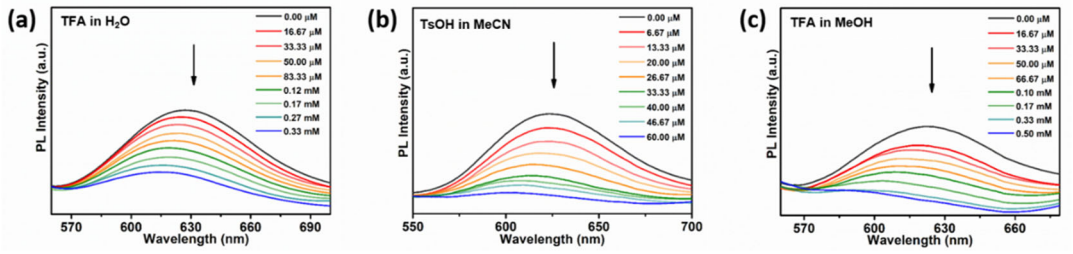

Figure S11. Fluorescence spectra of TPBD-TA COF in (a) TFA aqueous solution, (b) TsOH in MeCN solution, (c) TFA in MeOH solution with different acid concentration (λex = 365 nm).

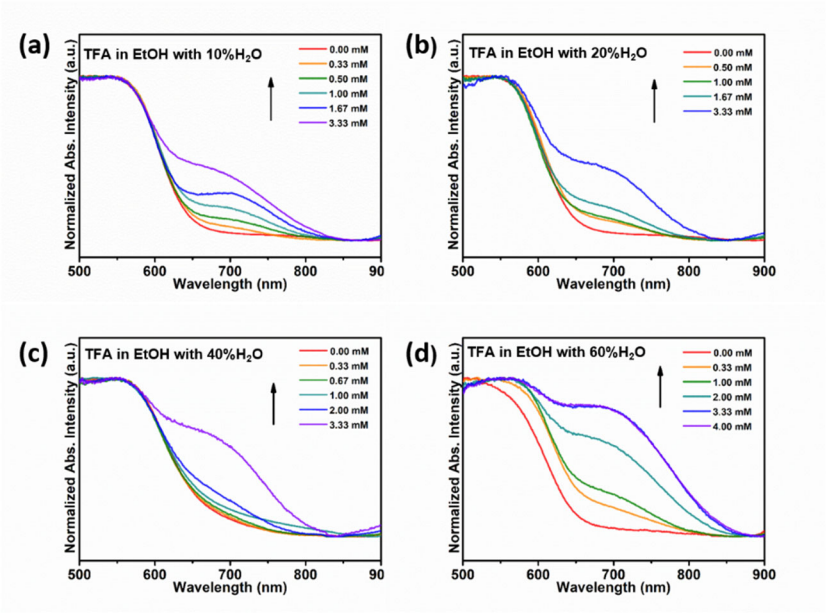

Figure S12. Solid-state absorption spectra of TPBD-TA COF in EtOH solution of TFA with various amounts of water (V/V): (a)10%, (b) 20%, (c) 40%, (d) 60% and different acid concentration.

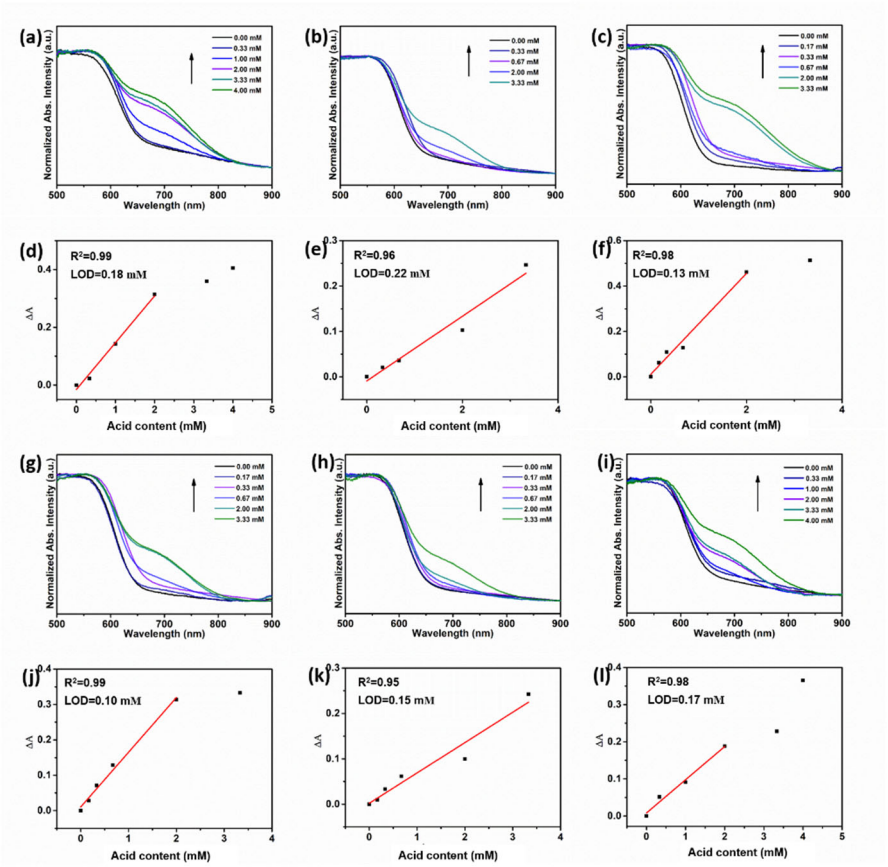

Figure S13. Solid-state absorption spectra of TPBD-TA COF in acetone solution of TFA with various amounts of water (V/V): (a) 5%, (b) 10%, (c) 20%, (g) 40%, (h) 60%, (i) 80%, (d-f) and (j-l) the linear correlation between the absorbance change ($\Delta A = A_{H^+} - A_{blank}$) with increasing concentration of acid in different solutions.

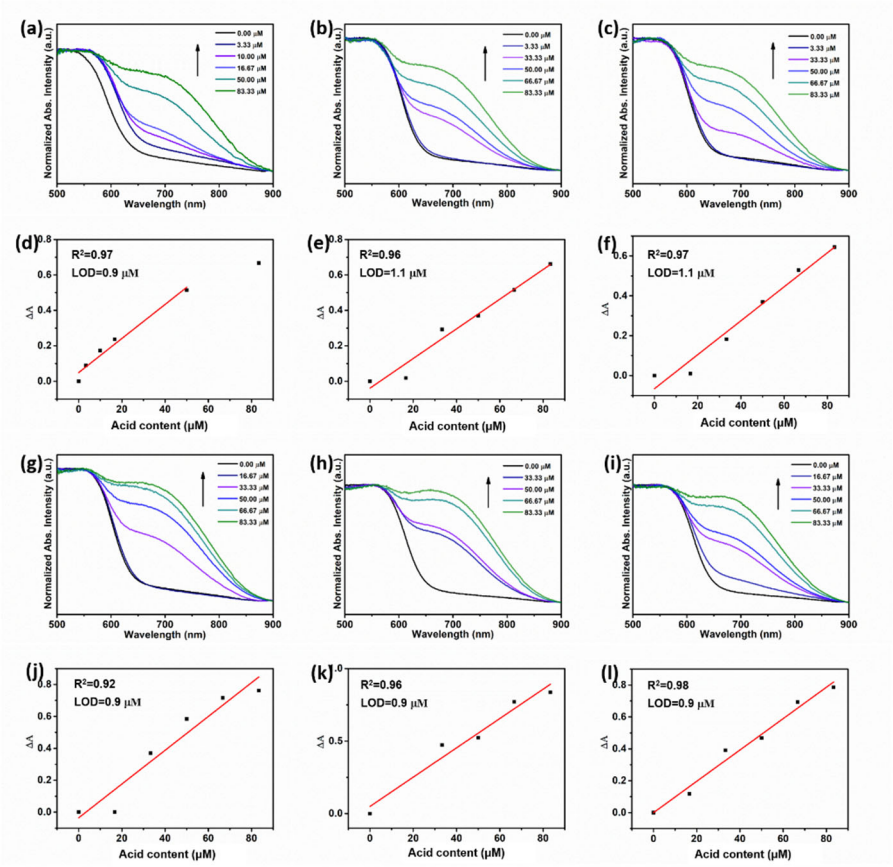

Figure S14. Solid-state absorption spectra of TPBD-TA COF in MeCN solution of TsOH with various amounts of water (V/V): (a) 5%, (b) 10%, (c) 20%, (g) 40%, (h) 60%, (i) 80%, (d-f) and (j-l) the linear correlation between the absorbance change ($\Delta A = A_{H^+} - A_{blank}$) with increasing concentration of acid in different solutions.

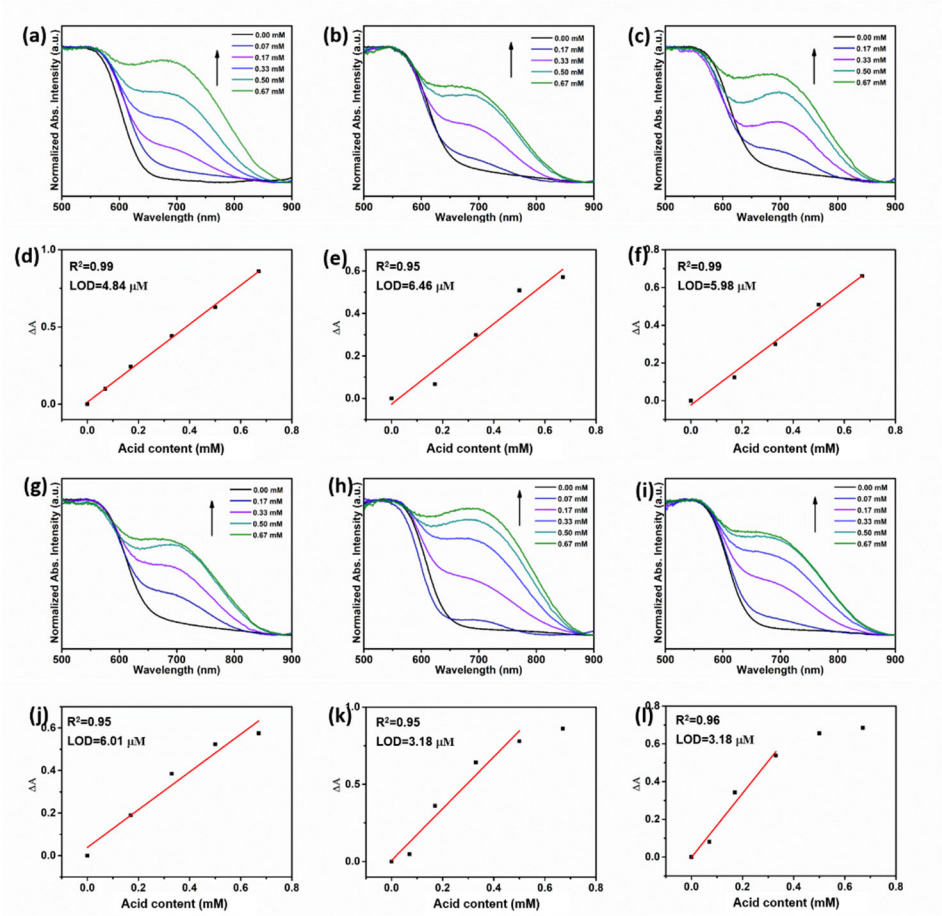

Figure S15. Solid-state absorption spectra of TPBD-TA COF in EtOH solution of TFMS with various amounts of water (V/V): (a) 5%, (b) 10%, (c) 20%, (g) 40%, (h) 60%, (i) 80%, (d-f) and (j-l) the linear correlation between the absorbance change ($\Delta A = A_{H^+} - A_{blank}$) with increasing concentration of acid in different solutions.

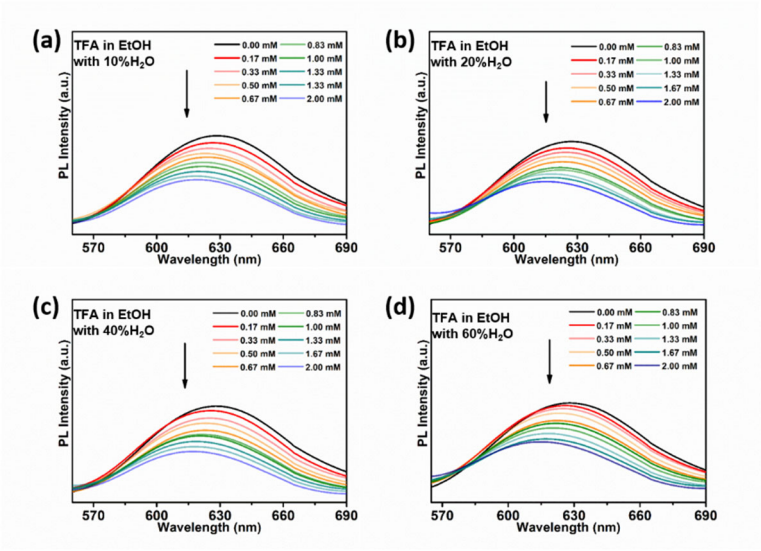

Figure S16. Fluorescence spectra of TPBD-TA COF in EtOH solution of TFA with various amounts of water (V/V): (a) 10%, (b) 20%, (c) 40%, (d) 60% and different acid concentration (λex = 365 nm).

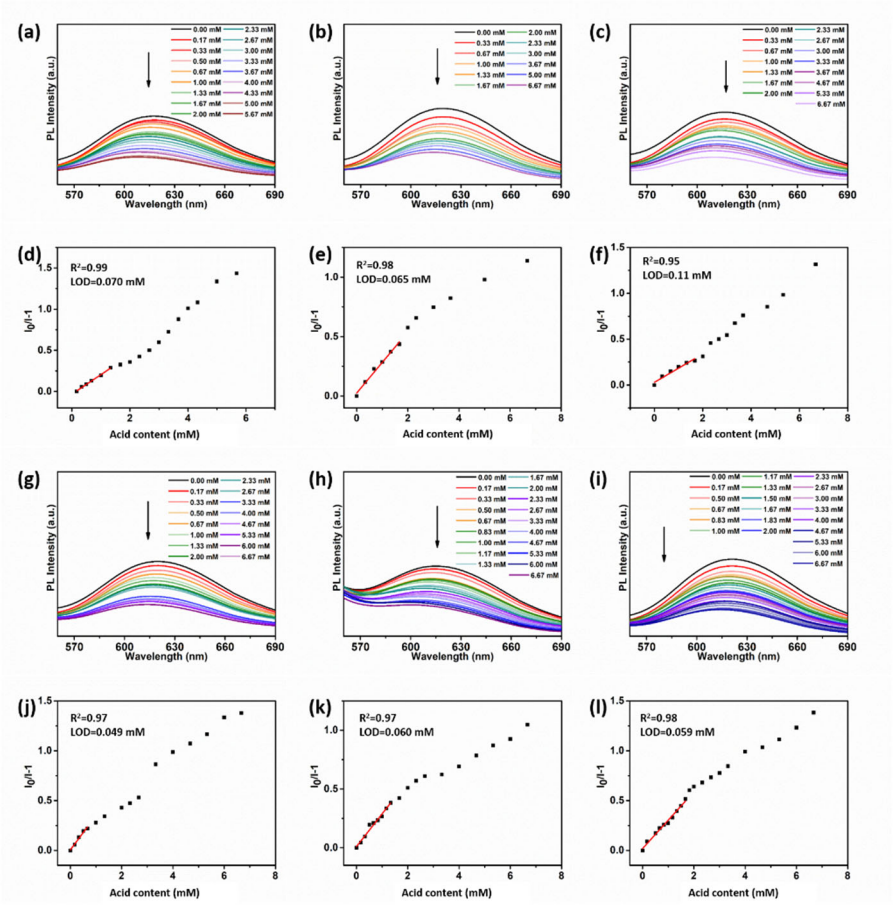

Figure S17. Fluorescence spectra of TPBD-TA COF in acetone solution of TFA with various amounts of water (V/V): (a) 5%, (b) 10%, (c) 20%, (g) 40%, (h) 60%, (i) 80%, (d-f) and (j-l) the linear correlation between the fluorescence change with increasing concentration of acid in different solutions (λex = 365 nm).

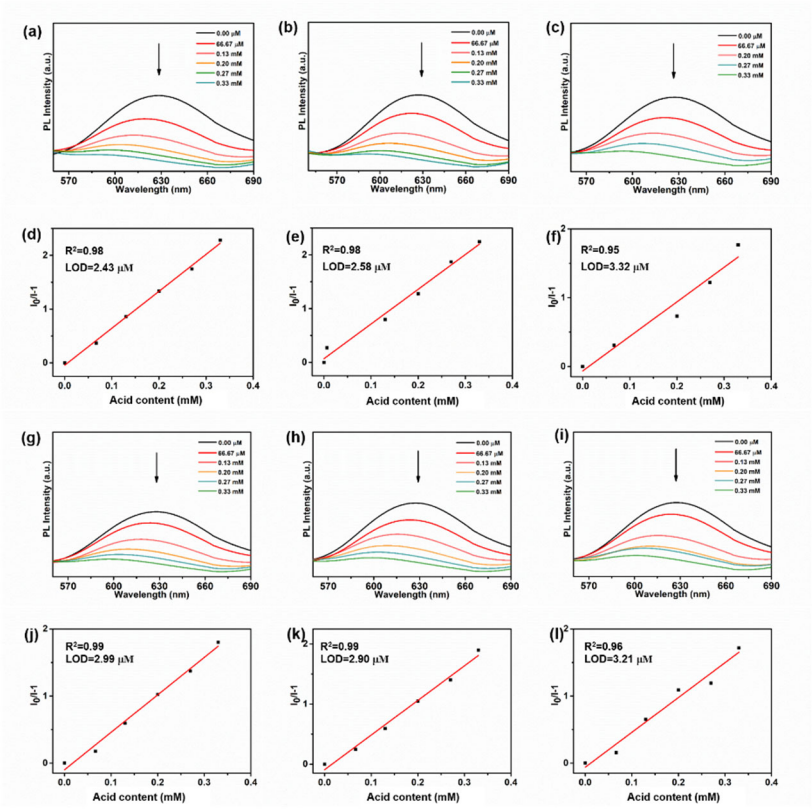

Figure S18. Fluorescence spectra of TPBD-TA COF in EtOH solution of TsOH with various amounts of water (V/V): (a) 5%, (b) 10%, (c) 20%, (g) 40%, (h) 60%, (i) 80%, (d-f) and (j-l) the linear correlation between the fluorescence change with increasing concentration of acid in different solutions (λex = 365 nm).

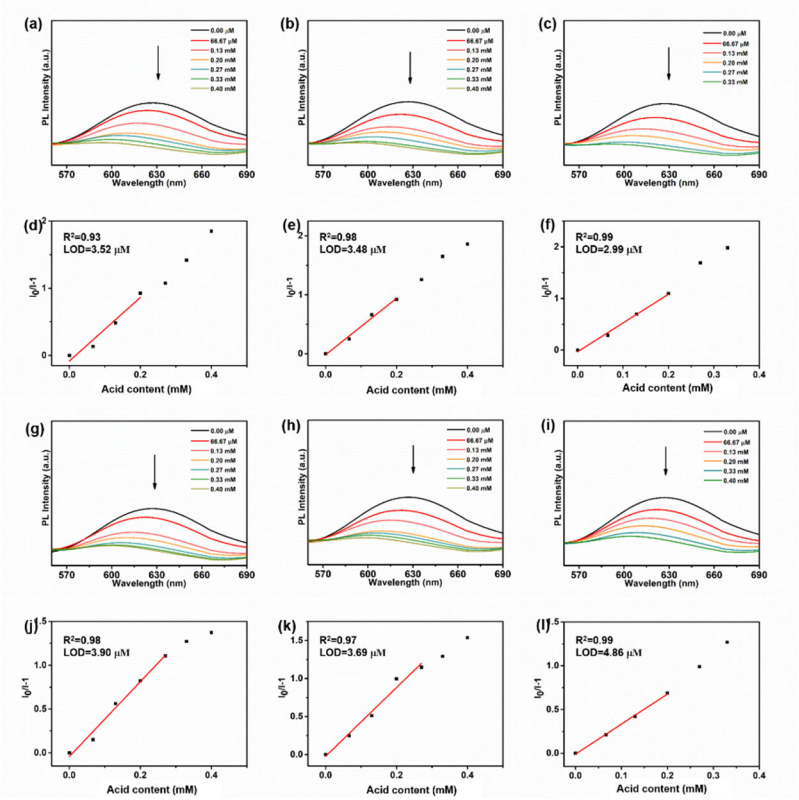

Figure S19. Fluorescence spectra of TPBD-TA COF in EtOH solution of TFMS with various amounts of water (V/V): (a) 5%, (b) 10%, (c) 20%, (g) 40%, (h) 60%, (i) 80%, (d-f) and (j-l) the linear correlation between the fluorescence change with increasing concentration of acid in different solutions (λex = 365 nm).

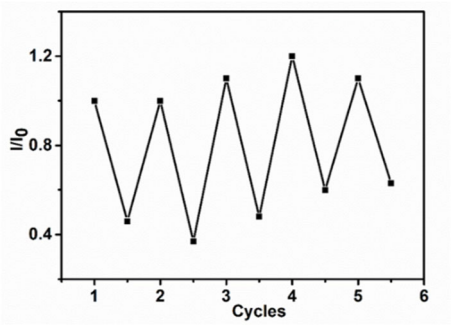

Figure S20. The repeatability of TPBD-TA COF for detecting TFA in EtOH solvent.

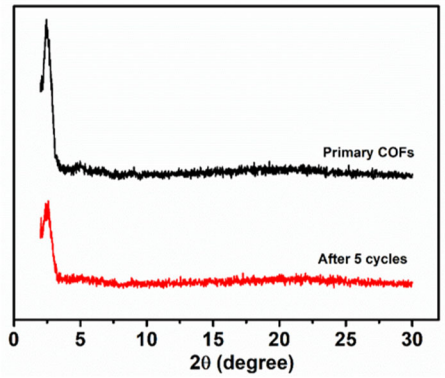

Figure S21. PXRD patterns of TPBD-TA COF for detecting TFA in EtOH solvent.

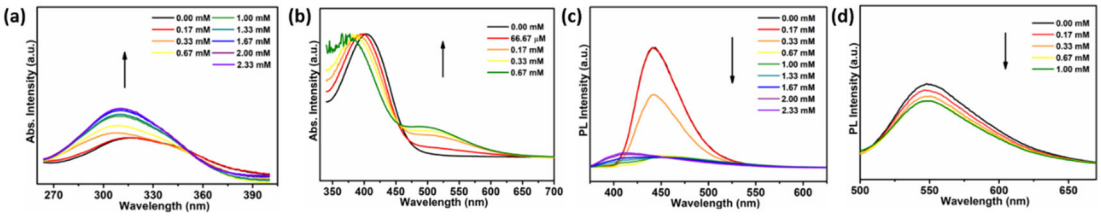

Figure S22. UV-vis absorption spectra of (a) TPBD and (b) the model compound in different concentrations of p-Toluenesulfonic acid (TsOH), fluorescence spectra of (c) TPBD and (d) the model compound in different concentrations of TsOH.

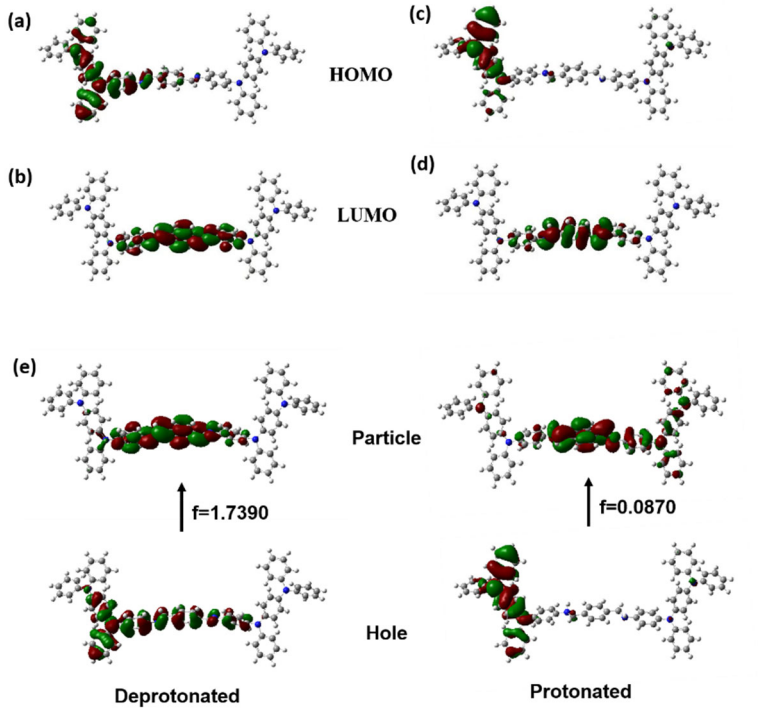

Figure S23. TD-DFT derived frontier orbitals contribution: (a) and (b) COF fragment in the deprotonated state, (c) and (d) in protonated state, (e) the natural transition orbitals (hole ones at the bottom and electron ones at the top) of the COF.

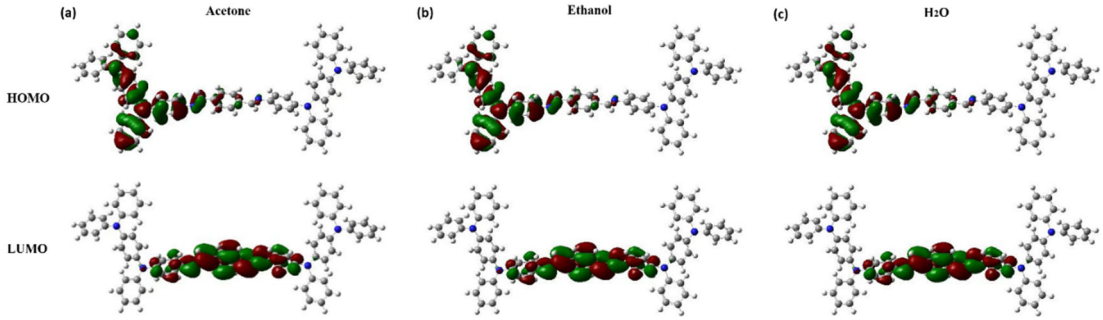

Figure S24. TD-DFT derived frontier orbitals contribution: the deprotonated COF fragment in (a) acetone, (b) ethanol and (c) H_2O.

Table S1. Comparation of acid detection of COF.

Materials	Detection Range	Limit of Detection	Detection Method	Solution Environment	Ref.
COF-TP	pH=0-6	———	Fluorescence	aqueous phase	ACS Appl. Mater. Interfaces 2021, 13, 1145−1151
VCOF-PyrBpy	pH =1-12	———	Fluorescence /Colorimetric	aqueous phase	ACS Appl. Mater. Interfaces
COF-HQ	pH=1-5	———	Fluorescence /Colorimetric	———	ACS Appl. Mater. Interfaces 2018, 10, 15364−15368
PyTA-BC-Ph COFs	———	20 nmol / L	Fluorescence		Adv. Optical Mater. 2020, 2000641
Per-N COF	35 μg /L -- 110 mg /L	———	Colorimetric	nonaqueous solutions	J. Am. Chem. Soc. 2019, 141, 15693−15699
COF-JLU4	pH =0.9–13.0	———	Fluorescence	water	Chem. Commun., 2016, 52, 11088--11091
TPBD-TA COF	———	**58 nmol / L / (0.4 μmol / L)**	**Fluorescence /Colorimetric**	**aqueous solutions and nonaqueous solutions**	**This work**

Table S2. Atomic coordinates of TPBD-TA COF for the AA-stackinig model.

C1	C	0.18255	0.41237	-0.10606
C2	C	0.2121	0.4082	-0.15455
C3	C	0.24396	0.42928	0.00083
C4	C	0.24574	0.4545	0.20737
C5	C	0.21616	0.45871	0.25569
C6	C	0.18433	0.43771	0.09926
C7	C	0.15341	0.44264	0.15027
C8	C	0.27495	0.42471	-0.05765
N9	N	0.00331	0.56782	1.01145
C10	C	-0.02916	0.56959	1.00287
C11	C	0.00168	0.53356	1.00642
C12	C	0.03732	0.60051	1.03066
C13	C	0.02873	0.52967	0.87065
C14	C	0.02704	0.49662	0.8635
C15	C	-0.03282	0.59421	1.1804
C16	C	-0.06438	0.5955	1.17755
C17	C	-0.09292	0.57239	0.99697
C18	C	-0.08942	0.54776	0.81632
C19	C	-0.05771	0.5466	0.81913
C20	C	0.06474	0.60262	1.21122
C21	C	0.0974	0.63432	1.23218
C22	C	0.10351	0.6645	1.07176
C23	C	0.07599	0.6627	0.89259
C24	C	0.04333	0.631	0.87289
N25	N	0.1376	0.69629	1.10267
N26	N	-0.12488	0.57455	1.01161
H27	H	0.15834	0.396	-0.23081
H28	H	0.21019	0.38873	-0.31608
H29	H	0.27004	0.4709	0.33107
H30	H	0.21807	0.47825	0.4164
H31	H	0.15527	0.46086	0.32321
H32	H	0.27308	0.4075	-0.2396
H33	H	0.05139	0.55232	0.77211
H34	H	0.04834	0.49471	0.75747
H35	H	-0.01135	0.61213	1.32375
H36	H	-0.06697	0.61427	1.31952
H37	H	-0.11076	0.52935	0.67367
H38	H	-0.05534	0.5277	0.67884
H39	H	0.06075	0.57969	1.33575
H40	H	0.11818	0.6356	1.37432

H41	H	0.07914	0.68546	0.76937
H42	H	0.02264	0.63027	0.7349

Unit Cell Parameters (P-3).

a = b = 43.35 Å, c = 4.46 Å.

α = β = 90°, γ = 120°.

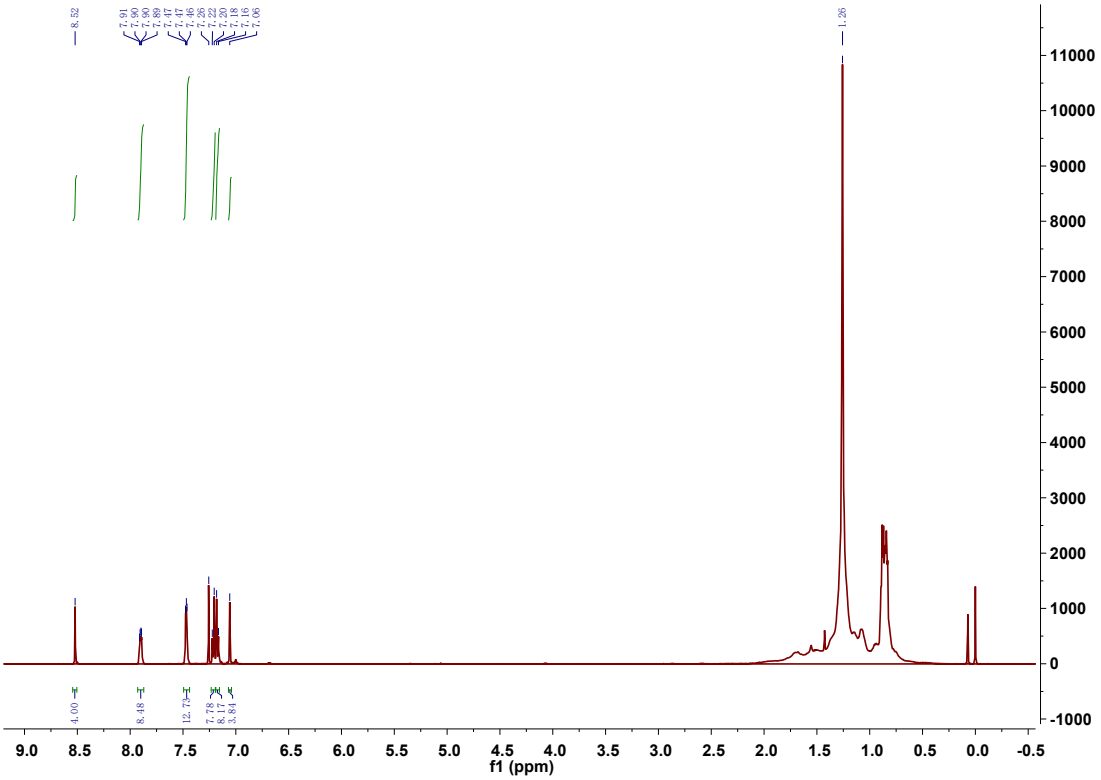

Figure S25. ^{1}H NMR spectrum of the model compound **(1)**.

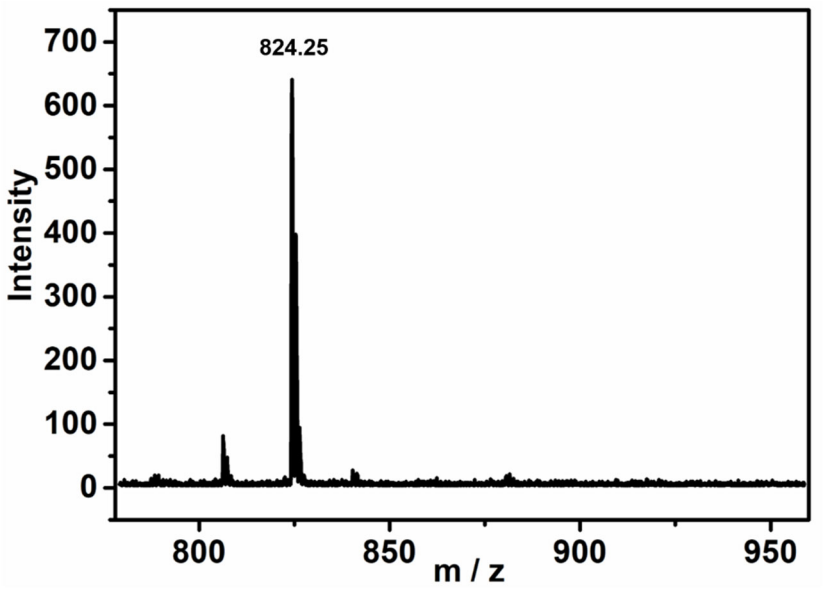

Figure S26. The MALDI-TOF mass spectrum of the model compound **(1) (**Calcd. for $C_{58}H_{44}N_6$: 824.36).

References

1. Hao, Q.; Li, Z.J.; Bai, B.; Zhang, X.; Zhong, Y.W.; Wan, L.J.; Wang, D. A Covalent Organic Framework Film for Three-State Near-Infrared Electrochromism and a Molecular Logic Gate. *Angew. Chem. Int. Edit.* **2021**, *60*, 12498–12503.
2. Grigoras, M.; Stafie, L. Synthesis and Characterization of Linear, Branched and Hyperbranched Triphenylamine-Based Polyazomethines. *Des. Monomers Polymers.* **2009**, *12*, 177–196.
3. M. J. Frisch, G. W. Trucks, H. B. Schlegel, G. E. Scuseria, M. A. Robb, J. R. Cheeseman, G. Scalmani, V. Barone, B. Mennucci, G. A. Petersson, H. Nakatsuji, M. Caricato, X. Li, H. P. Hratchian, A. F. Izmaylov, J. Bloino, G. Zheng, J. L. Sonnenberg, M. Hada, M. Ehara, K. Toyota, R. Fukuda, J. Hasegawa, M. Ishida, T. Nakajima, Y. Honda, O. Kitao, H. Nakai, T. Vreven, J. A. Montgomery, Jr., J. E. Peralta, F. Ogliaro, M. Bearpark, J. J. Heyd, E. Brothers, K. N. Kudin, V. N. Staroverov, T. Keith, R. Kobayashi, J. Normand, K. Raghavachari, A. Rendell, J. C. Burant, S. S. Iyengar, J. Tomasi, M. Cossi, N. Rega, J. M. Millam, M. Klene, J. E. Knox, J. B. Cross, V. Bakken, C. Adamo, J. Jaramillo, R. Gomperts, R. E. Stratmann, O. Yazyev, A. J. Austin, R. Cammi, C. Pomelli, J. W. Ochterski, R. L. Martin, K. Morokuma, V. G. Zakrzewski, G. A. Voth, P. Salvador, J. J. Dannenberg, S. Dapprich, A. D. Daniels, O. Farkas, J. B. Foresman, J. V. Ortiz, J. Cioslowski, and D. J. Fox, Gaussian 09, Revision D.01, Gaussian, Inc.: Wallingford CT, USA2009.